Scanning Microscopy

Volume 9 | Number 3 Article 17

6-28-1995

The Interaction of Laser Energy with Ureter Tissues in a Long Term Investigation

U. Stratmann
University of Munster

K. Schaarschmidt
University of Munster

R. R. Lehmann
University of Munster

A. Heinze
Central Laser Laboratory, Neuherberg

G. H. Willital
University of Munster

See next page for additional authors

The Interaction of Laser Energy with Ureter Tissues in a Long Term Investigation

Authors

U. Stratmann, K. Schaarschmidt, R. R. Lehmann, A. Heinze, G. H. Willital, and E. Unsold

Scanning Microscopy, Vol. 9, No. 3, 1995 (Pages 805-816) 0891-7035/95$5.00+.25
Scanning Microscopy International, Chicago (AMF O'Hare), IL 60666 USA

THE INTERACTION OF LASER ENERGY WITH URETER TISSUES IN A LONG TERM INVESTIGATION

U. Stratmann[1,*], K. Schaarschmidt[2], R.R. Lehmann[1], A. Heinze[3], G.H. Willital[2] and E. Unsöld[3]

[1]Institute of Anatomy, [2]Clinic of Pediatric Surgery, University of Münster, Germany
[3]GSF, Central Laser Laboratory, Neuherberg, Germany

(Received for publication August 22, 1994, and in revised form June 28, 1995)

Abstract

This study investigates tissue responses after laser irradiation of the rabbit ureter, which serves as an experimental model for rectourogenital fistulae of children. Twenty-five rabbit ureters were irradiated intraluminally by a Nd:YAG laser 1320 nm (2 Watt, 20 seconds and 3 Watt, 8 seconds) via an applicator with radialsymmetrical light distribution. Immediately, 2 weeks, 4 weeks, 8 weeks, and 16 weeks after irradiation, the ureters were X-rayed with contrast solution and prepared for light and transmission electron microscopy. For the parameters employed, no apparent morphological differences could be observed. Immediately, the central laser zone showed a transmural thermonecrosis prevailed by cellular destruction, condensed ground substance and occlusion of most vascular lumina. Peripheral laser zones displayed urothelial vacuolations. Between 2 and 16 weeks, urothelial regeneration and ingrowth of granulation tissue caused a luminal stenosis or occlusion followed by transformation into scar tissue. In some peripheral laser zones, a hydroureter with marked luminal dilatation developed. We conclude that the ureter is occluded if the expanding force of the growing scar tissue exceeds the hydrostatic pressure of the obstructed urine. A laser occlusion of rectourogenital fistulae will be easier to achieve since fistula occlusion does not entail an obstruction of the urine flow.

Key words: Nd:YAG laser, rabbit ureter, rectourogenital fistula, immediate tissue response, thermal necrosis, healing process, luminal occlusion, hydroureter, ultrastructure, radiology

*Address for correspondence:
Udo Stratmann
Institute of Anatomy
University of Münster
Robert Koch Straße 26
D-48129 Münster, FRG
Telephone number: 49-251-835198
FAX number: 49-251-835241

Introduction

Urology is one of the first clinical fields in which the clear superiority of laser treatment to other therapeutic regimens has been proven and standard indications for laser treatment have been defined. Hofstetter and Keiditsch (1986), Keiditsch (1986), and Grossman *et al.* (1992) could show that endoscopic transmural laser coagulation of the bladder or ureter wall was a curative treatment for disseminated bladder cancer and cancer of the ureter and could spare many patients a cystectomy or ureteral resection. Another clinical laser application in the urogenital tract is the ureteroscopic laser-lithotripsy of large ureteral calculi (Schmidt-Kloiber *et al.*, 1985), a process which avoids major surgical procedures in many patients.

In children, the use of laser-urology has just recently begun [e.g., for cutting congenital urethral valves in inferior urinary obstruction or for partial nephrectomy in bilateral nephroblastoma (Shearer *et al.*, 1993)]. A number of recent experimental studies have been conducted in order to develop further clinical laser applications in the urinary tract (Merguerian and Rabinowitz, 1986; Zimmermann and Kraushaar, 1987; Burger *et al.*, 1990; Salo *et al.*, 1992).

The purpose of the current study was to clarify the morphology, the mechanism and the feasibility of occlusion of hollow organs by intraluminal laser radiation. This was performed with the aim of establishing the biological basis for future occlusion of rectourogenital fistulae in newborn children suffering from anorectal atresia by a laserendoscopic procedure. An early minimally invasive occlusion of these rectourogenital fistulae would help to prevent renal damage from recurrent ascending urinary infections which is an inherent risk of current primary therapy by colostomy.

We, therefore, chose the rabbit ureter as an analogous animal model to simulate the clinical situation and conducted a morphological long-term investigation on the chronological sequence of ureteral tissue reactions to standardized intraluminal laser radiation and its repair mechanisms in up to 16 postoperative weeks.

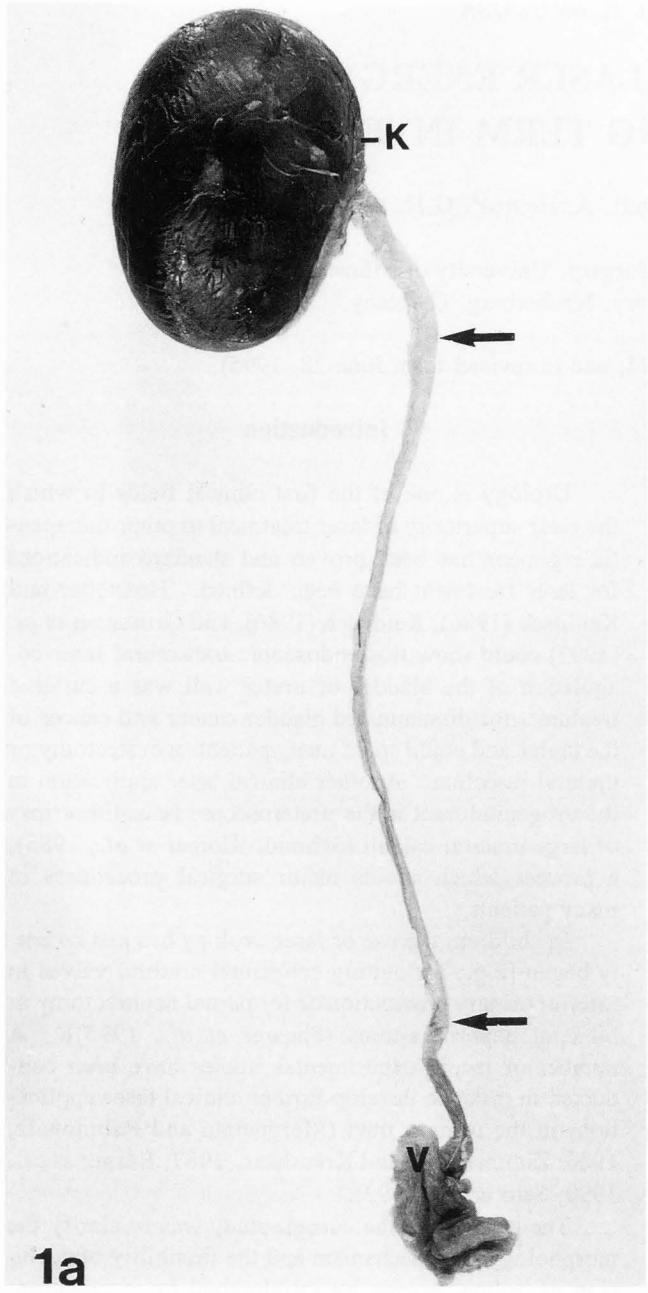

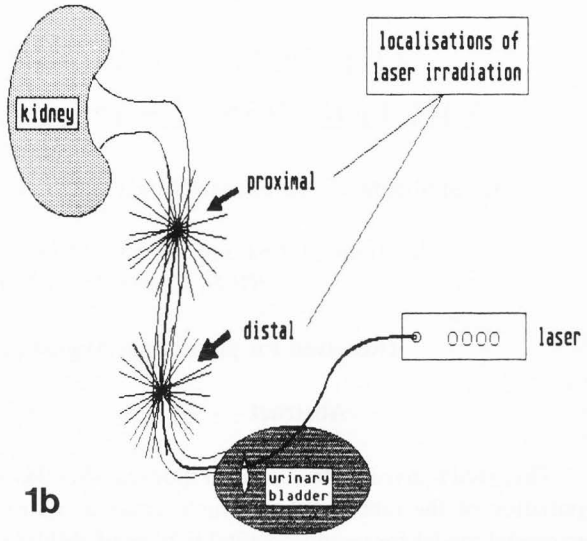

Figure 1. (a) Macroscopic photograph of a freshly dissected right upper urinary tract of the rabbit. K: kidney; V: segment of the urinary bladder; arrows: localisation of the intraluminal laser irradiation. Bar = 1 cm. (b) Diagram of the urinary tract with inserted laser fibre and schematic indication of the proximal and distal site of laser application.

Materials and Methods

After a premedication with 0.5 mg/kg of atropine and 0.2 mg/kg prothypendyl-HCl, white New Zealand rabbits were anaesthetised by isoflurane/oxygen-inhalation (5%) via a face mask. From a lower midline laparotomy, the anterior bladder wall was opened and the right ureter ostium was cannulated by a 430 μm laser fibre equipped with a new radial laser applicator at its tip.

The laser fibre was advanced in a retrograde direction towards the pelvis of the right kidney. The proximal site of irradiation was located in the upper third of the ureter and the distal site of irradiation was located in the lower third (Figs. 1a and 1b). The new radial applicator was designed to ensure a radialsymmetrical distribution of light and an irradiation of a definite circumferential volume of the ureteral wall. We used a Nd:YAG laser (wavelength: 1320 nm) with continuous light emission to irradiate both sites with alternating laser parameters, i.e., 2 watt and 20 seconds or 3 watt and 8 seconds. Suitable parameters for achieving moderate but not transmural wall necrosis (to prevent wall perforation) were determined by previous experiments and evaluated by thermography and histomorphometry. Thermographically, it was our aim not to surpass a maximum temperature of 60°C in the centre of irradiation, whereas the depth and the extension of the coagulated zone was evaluated by histomorphometry. After laser treatment, the abdominal wound was closed in layers and, postoperatively, the animals received normal oral nutrition and water *ad libitum*.

The morphological tissue response was examined in groups of 5 animals: immediately, 2 weeks, 4 weeks, 8 weeks, and 16 weeks after laser irradiation. The contralateral left ureter served as an internal control. At the time of operation, the control ureters underwent a laser fibre cannulation without laser-irradiation.

After reaching the given postoperative intervals the animals were anaesthetised and fixed by perfusion with glutaraldehyde (2.5% in 0.1 M phosphate buffer, 4°C, pH 7.2). The laser treated ureters as well as the control

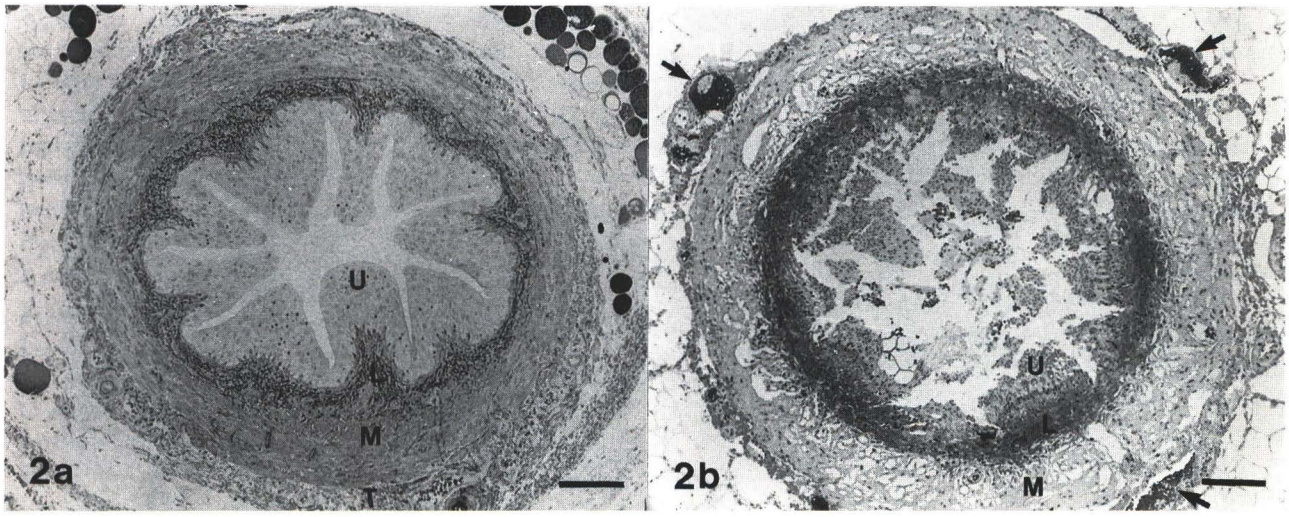

Figure 2. (a) Light micrograph of a cross-sectioned control rabbit ureter. U: urothelium; L: cell-rich and cell-poor zone of lamina propria; M: muscularis; T: tunica adventitia. Toluidine blue. Bar = 160 μm. (b) Light micrograph of a cross-sectioned rabbit ureter from the central laser zone immediately after laser irradiation (Nd:YAG 1320 nm 3 Watts / 8 seconds). U: destroyed urothelium; L: condensed lamina propria; M: damaged muscularis; arrows: occluded blood vessels in the tunica adventitia. Toluidine blue. Bar = 160 μm.

ureters were dissected, filled with a cooled mixture (4°C) of contrast solution and glutaraldehyde (1:1, Ultravist 300 Schering; 5% glutaraldehyde) and X-rayed after immersion in a 2.5% solution of glutaraldehyde.

For histological investigation, we cut both irradiated sites in the middle of their laser zones in a transversal direction. The laser zone could easily be identified macroscopically by a whitish coloured wall segment in the immediate group or by the development of a hydroureter in the postoperative groups. The sectioned pieces were post-fixed by 1% OsO_4 buffered with 0.1 M cacodylate (pH 7.2), dehydrated and embedded in Epon 812. From the embedded pieces, 3 segments of the laser zone were cut in steps of 2 mm distance:

Segment 1: 0-2 mm from the middle of laser zone
Segment 2: 2-4 mm from the middle of laser zone
Segment 3: 4-6 mm from the middle of laser zone

Below, segment 1 will be termed as the central laser zone, whereas segments 2 and 3 will be referred to as peripheral laser zones. From each segment, semi-thin sections (stained with toluidine blue) were used for light microscopy (LM) and successive ultrathin sections (stained with uranyl acetate and lead citrate) were processed for transmission electron microscopical (TEM) evaluation.

For computer aided semi-quantitative planimetry, the light micrographs were digitized by means a TV-camera and the data were entered into an automatic image analysis system (IBAS, Contron Ltd., Düsseldorf, Germany) equipped with a morphometrical program for planimetry (area measurement). Thereby, the luminal area of each ureter cross-section was manually outlined on the digitizing tablet and then the residual luminal area was compared with the contralateral control ureter.

Table 1. Survey of groupings and sizes.

design of the study	number
total animals	25
animals per group	5
irradiated ureters	25
control ureters	25
irradiated ureter sites	50
sections/irradiated ureter site	6
sections of irradiated ureters	300
sections/control ureter	2
sections of control ureters	50
sections/animal	14
total sections	350

Statistical analysis of the data was performed by the SAS statistic program via an analysis of variance (Scheffe-test for pair-wise comparison, level of significance: $p \leq 0.05$). This was preceded by a Proc Univariate procedure for testing the normal distribution of data. Thus, the grade of stenosis could be classified semi-quantitatively as slight, moderate or severe. Table 1 gives a survey of the design of the study.

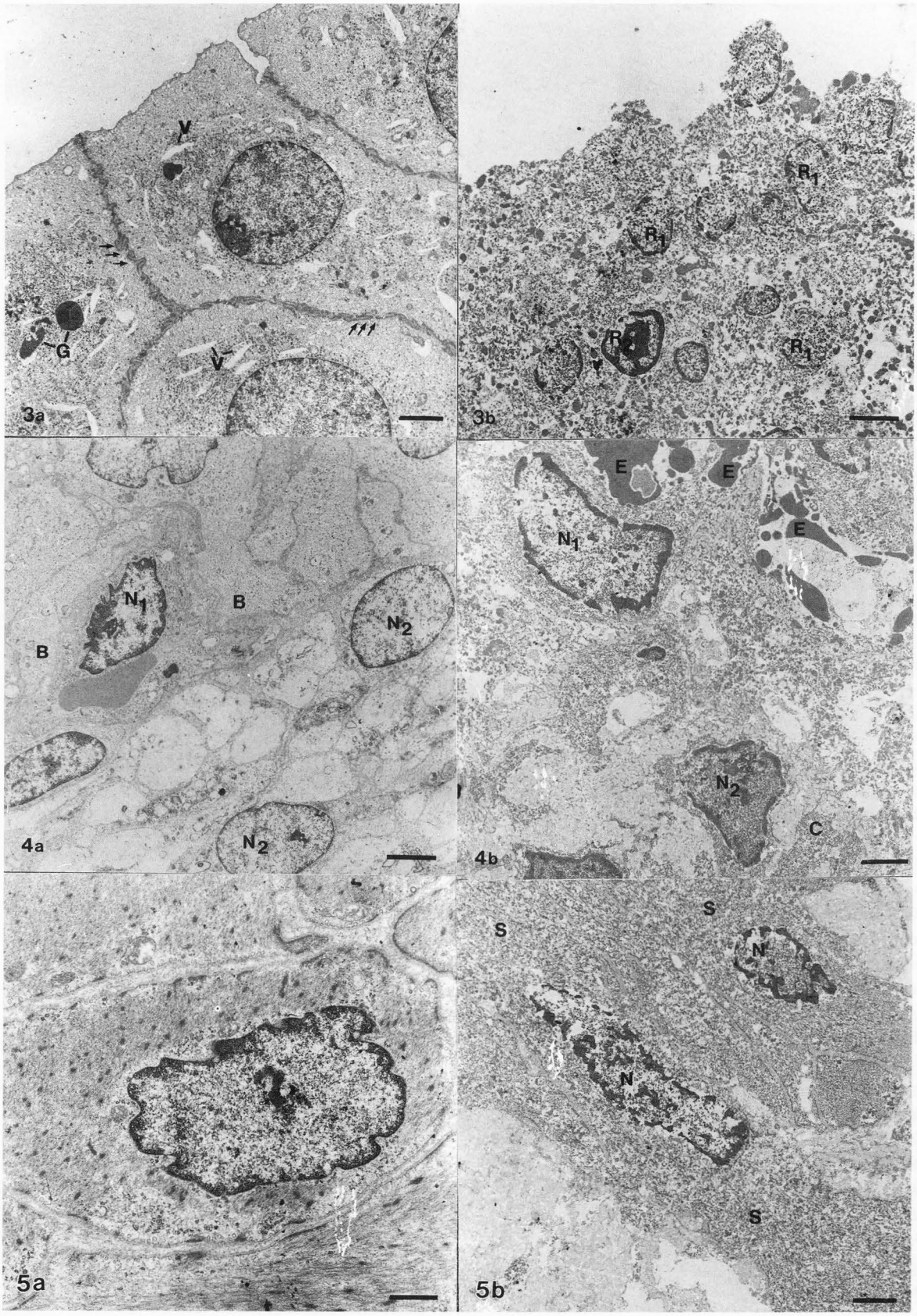
V
G
V
3a
R1
R1
R1
R1
3b
N1
B
B
N2
N2
4a
E
E
E
N1
N2
C
4b
S
S
N
N
S
5a
5b

Figure 3. Electron micrographs of superficial cells in the urothelium of a rabbit ureter. (a) Control ureter. G: dark granules; V: lenticular vesicles; arrows: lateral interdigitations (note abundant free ribosomes in the cytoplasm. Bar = 1 μm. (b) Ureter immediately after laser irradiation (Nd:YAG 1320 nm, 3 Watts / 8 seconds). R_1: karyolytic remnants of nuclear fragments; R_2: pycnotic like remnant of a nuclear fragment. Bar = 1 μm.

Figure 4. Electron micrographs of cells in the stratum basale and in the lamina propria of a rabbit ureter. (a) Control ureter. B: portion of a basal cell of the urothelium; N_1: endothelial nucleus of a capillary protruding from the lamina propria; N_2: nucleus of stellate reticular-like cell in the cell-rich zone of the lamina propria. Bar = 1 μm. (b) Ureter immediately after laser irradiation (Nd:YAG 1320 nm 3 Watts / 8 seconds). E: fragmented erythrocytes in a capillary lumen between the basal cells of the urothelium; N_1: endothelial nucleus of the same capillary; N_2: nucleus of a connective tissue cell in a condensed lamina propria; C: cytoplasmic process of connective tissue cell. Bar = 1 μm.

Figure 5. Electron micrographs of a cross-sectioned smooth muscle cell in the muscularis of a rabbit ureter. (a) Control ureter. (Note numerous dense areas in the sarcoplasm and peripheral caveoli). Bar = 1 μm. (b) Ureter immediately after laser irradiation (Nd:YAG 1320 nm 3 Watts / 8 seconds). N: pycnotic-like nucleus; S: destroyed sarcoplasm. Bar = 1 μm.

Results

Morphological findings in the control ureter

Cross-sections of control ureters showed the typical stellate lumen with prominent longitudinal mucosal folds (Fig. 2a). The transitional epithelium (urothelium) was composed of a stratum basale, a stratum intermedium and a stratum superficiale. It could be classified as a stratified epithelium and consisted of 12-15 cell layers.

TEM observations of the stratum superficiale (Fig. 3a) did not display all structural features peculiar to these cells in other species as the flattened lenticular vesicles were not bounded by a thick membrane of the same character as that on the free luminal surface. Furthermore, the distribution of these vesicles was not confined to the apical portions of the superficial cells.

Additionally, we could observe dark granules with a homogeneous electron-dense content which were distributed throughout all cell layers of the urothelium and could already be described light microscopically. At the lateral cell borders numerous interdigitations were visible. The most prominent feature of the stratum basale were numerous capillary loops protruding from subepithelial vessels of the lamina propria (Fig. 4a). The underlying lamina propria was composed of 2 structurally different zones (Fig. 2a).

By the TEM, the first cell-rich zone comprised a 5-10 μm wide superficial layer with stellate reticular-like cells exhibiting numerous cytoplasmic processes and connected to each other by a three-dimensional network (Fig. 4a). The intercellular spaces were filled with abundant amorphous ground substance devoid of collagenous fibrils or elastic material.

The second cell-poor zone comprised a 10-15 μm wide deep layer with a high portion of fibre bundles arranged in an irregular texture. Few fibroblasts and fibrocytes were interspersed between the mesh of this fibrous feltwork traversed by small blood vessels. A distinct submucosal layer could not be identified in the rabbit ureter.

In the muscularis, 3 distinct smooth muscle layers could be discerned. Fine inner and outer layers contained isolated bundles of longitudinally arranged muscle cells, whereas the stronger, intermediate layer displayed a coherent mass of muscle fibres with a predominantly circular course (Fig. 2a). The smooth muscle cells of the 3 layers were sustained by copious loose connective tissue. The tunica adventitia (Fig. 2a) could be described as a layer of loose connective tissue with large vessels and nerve fibres neighbouring the adipose tissue of the retroperitoneal space.

Morphological findings immediately after laser irradiation

Immediately after laser irradiation apparent differences in the morphological tissue response could not be determined for the 2 chosen combinations of parameters (2 Watts / 20 seconds and 3 Watt / 8 seconds). The morphological differences compared to the control ureters were most prominent in segment 1. Light microscopically, the stellate lumen of the ureter was no longer recognizable as the mucosal folds had been destroyed. The continuity of the transitional epithelium had completely disappeared due to a fragmentation and a detachment of fragments from persisting urothelial residues. In the destroyed urothelium, clear cell borders could no longer be discerned, and the nuclei seemed to be replaced by an obviously increased number of small and densely stained particles (Fig. 2b).

On the electron microscopical level, the cytoplasmic matrix, the organelles, the vesicles and granules as well as the cellular membranes showed complete disintegration and therefore did not allow distinction between the 3 different strata of the urothelium. Instead, we observed that the cytoplasmic structure had been entirely replaced by an inhomogeneous granulofilamentous material (Figs. 3b and 4b).

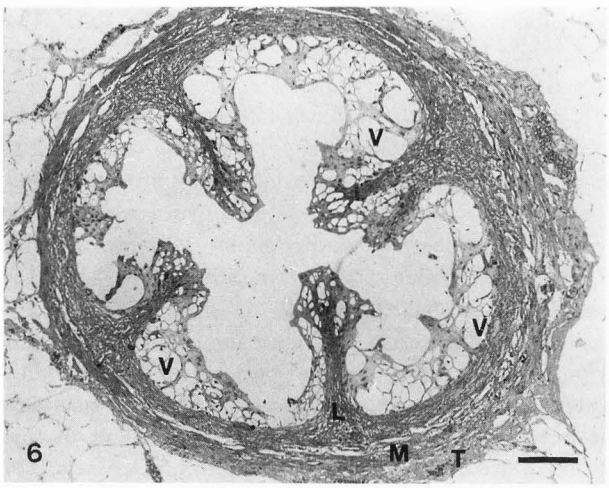

Figure 6. Light micrograph of a cross-sectioned rabbit ureter at a distance of 3 mm from the central laser zone immediately after laser irradiation (Nd:YAG 1320 nm 3 Watts / 8 seconds). V: numerous vacuoles in the destroyed urothelium; L: lamina propria, M: damaged muscularis; T: tunica adventitia. Toluidine blue. Bar = 160 μm.

Most urothelial nuclei presented either dense or pycnotic-like chromatin areas or karyolytic features (Fig. 3b). The nuclei showed both a remarkable decrease in diameter and a clear increase in number compared to the controls. The nuclear shrinkage and multiplication of this extent implies that the particles are residues of nuclear fragment rather than residues of whole nuclei.

Conversely, the endothelial nuclei of the capillary loops interposed between the basal cells showed no obvious signs of shrinkage but a disruption of the nuclear borders combined with thickened marginal chromatin and a coarse euchromatin. The lumina of the capillary loops interposed between the basal cells were filled with fragments of erythrocytes (Fig. 4b).

By the TEM, the cells of the lamina propria exhibited the same degree of cytoplasmic damage as already described for the urothelium. The nuclei of the connective tissue cells in the lamina propria were very similar in appearance to the endothelial nuclei of the capillary loops.

The amorphous ground substance of intercellular spaces in the cell-rich zone of the lamina propria had a more homogenous and more electron-dense ultrastructure than in the control ureters and could be best described as a condensed mass (Fig. 4b). The collagenous fibrils of the connective tissue were still visible, but were hardly detectable due to the surrounding condensed ground substance.

Light microscopically, the 2 zones of the lamina propria were indistinguishable and were replaced by an intensely stained dense circle of fused connective tissue components below the destroyed urothelium (Fig. 2b). The muscularis and the tunica adventitia appeared less severely damaged than the lamina propria and the urothelium, but differed from the controls by a loosened structure of their tissues and the features of their nuclei which seemed pycnotic in the connective tissue cells and the smooth muscle cells (Fig. 2b).

By the TEM, the sarcoplasm of the smooth muscle cells was devoid of myofilaments, dense areas and peripheral caveoli as seen in the controls (Fig. 5a) and showed transformation into the same inhomogeneous granulo-filamentous network observed in urothelial and connective tissue cells (Fig. 5b). The nuclei of the smooth muscle cells displayed the typical signs of structural damage already described for the endothelial and connective tissue cell nuclei.

A further striking observation of immediate tissue reaction to laser irradiation was the complete occlusion of almost all blood vessel lumina predominantly evident in the tunica adventitia (Fig. 2b). The occlusive material was intensely stainable in the light microscopical observation and was composed of blood cell aggregates embedded in a coagulation thrombus.

In segment 2 (2-4 mm from the middle of the laser zone), the ureter wall tissues showed the same qualitative lesions as described in segment 1 apart from the urothelium. Here, a multiple vacuolation of persisting urothelial residues was prominent (Fig. 6). These vacuoles were surrounded by a destroyed urothelium exhibiting the same ultracytological alterations as the one in segment 1.

The mucosal folds were preserved in segment 2 although the lamina propria did not yet allow distinguishing between 2 different zones and showed a fused, but not intensely stained tissue structure. Both light- and electron-microscopically, the muscularis and the tunica adventitia did not exhibit clear histological differences in comparison to segment 1, and the occlusion of blood vessel lumina was still evident.

In the more peripheral laser zone of segment 3 (4-6 mm from the middle of the laser zone), we did not find sufficient structural signs of a less severe damage of the ureter wall tissues, and therefore could not describe a gradient of decreasing laser destruction towards the distant wall segments.

Morphological findings in the period of 2-16 weeks after laser irradiation

Two weeks after laser irradiation the residues of the necrotic urothelium had detached from the underlying lamina propria and had been replaced by a regenerated

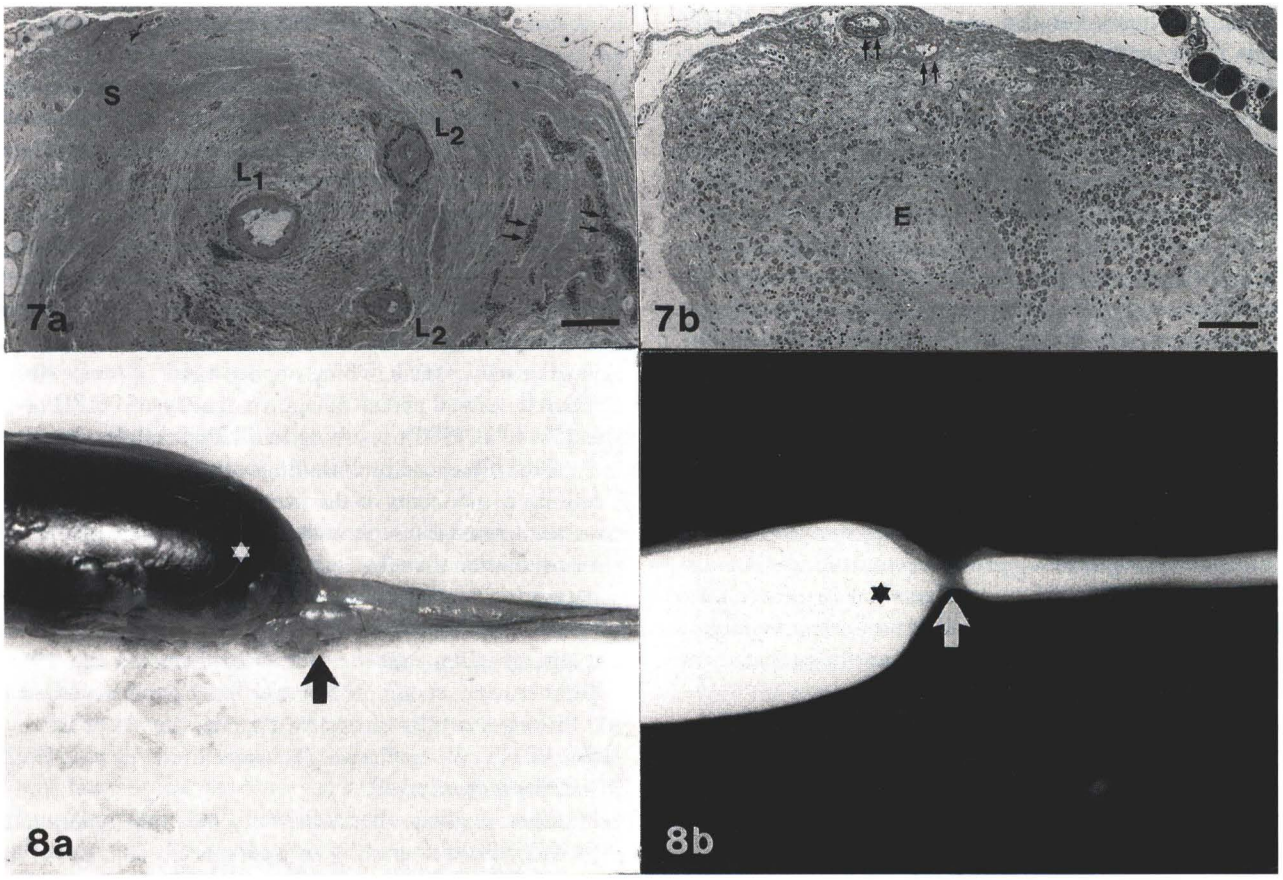

Figure 7. Light micrographs of a cross-sectioned rabbit ureter from the central laser zone 2 weeks after laser irradiation (Nd:YAG 1320 nm 3 Watts / 8 seconds). **(a)** L_{1-3}: stenosed lumina lined by regenerated urothelium; S: young scar tissue; arrows: longitudinally sectioned blood vessels in the region of the tunica adventitia. Toluidine blue. Bar = 160 μm. **(b)** E: central epithelial cells occluding the lumen; arrows: patent blood vessel in the tunica adventitia (note numerous macrophages interspersed between young scar tissue). Toluidine blue. Bar = 160 μm.

Figure 8. **(a)** Macroscopic photograph of a freshly dissected right rabbit ureter two weeks after laser irradiation of the proximal site (Nd:YAG 1320 nm 3 Watts / 8 seconds). Asterisk: hydroureter; arrow: central laser zone. Bar = 0.25 cm. **(b)** Contrast radiograph of the ureter shown in Figure 8a, two weeks after laser irradiation of the proximal site (Nd:YAG 1320 nm 3 Watts / 8 seconds). Asterisk: contrast solution filling hydroureter; arrow: weak radiopacity of young scar tissue occluding the lumen. Bar = 0.25 cm.

---

new urothelium in all 3 segments (Fig. 7a). This urothelium did not exhibit the typical cytological features of the controls and was therefore regarded as undifferentiated. It consisted of fewer cell layers (3-6) than the control urothelium (5-12 cell layers) and did not yet allow a distinction among a stratum basale, a stratum intermedium and a stratum superficiale.

The remaining wall layers, i.e., lamina propria, muscularis and tunica adventitia, could no longer be distinguished from one another due to an ingrowth of granulation tissue which had already been transformed into young scar tissue after 2 weeks. In segment 1, the expansion of the reparative connective tissue had caused a luminal stenosis in five of eight laser irradiated sites (62.5%). This stenosis was occasionally apparent as two or three residual lumina, separated by bridges of young scar tissue as shown in Figure 7a.

The grade of luminal stenosis was determined by comparing the luminal area to that of the controls, making use of semiquantitative planimetry. This technique allowed a rough classification into a low, intermediate and a high grade of stenosis. In the group of the stenosed specimens, all 3 grades of stenosis were found to occur. In the remaining 3 ureter sites (37.5%), a total occlusion of the lumen was apparent. However, the structural correlate of this occlusion was not only the

young scar tissue but also an accumulation of epithelial cells in the centre of the former lumen. In 2 of the occluded specimens, we found a high portion of macrophages interspersed between the surrounding young scar tissue in segment 1 (Fig. 7b) as a sign of recent or ongoing resorptive activity. After 2 weeks, most large blood vessels of the tunica adventitia had regained a patent lumen (Figs. 7a and 7b). In the peripheral laser zones of segment 2 and 3, all occluded ureter sites had developed a significant degree of luminal dilatation at the proximal site of laser irradiation (Figs. 8a and 8b), whereas a hydroureter at the distal site was only noticeable in a few cases.

Four weeks after laser irradiation, we detected no further expansion of the scar tissue and, therefore, no further increase in the number of luminal occlusions. At that instant, 25% of the irradiated sites showed luminal-occlusion in segment 1, while the remaining sites displayed all 3 grades of luminal stenosis. In the occluded specimens, central epithelial cell accumulations could no longer be detected because the scar tissue had now completely filled the former lumen.

Eight weeks after laser irradiation, we observed a gradual maturation of the scar tissue in the occluded specimens of segment 1. This structural alteration was characterized by an increase in the portion of fibres and a decrease in the portion of connective tissue cells as well as in the amount of ground substance. After 8 weeks, 38% of the irradiated sites showed luminal occlusion in segment 1. The stenosed specimens displayed only low and intermediate grades of stenosis.

Sixteen weeks after laser irradiation a shrinkage of the scar tissue had caused an obvious wall stricture of the central laser zone; this became particularly apparent by the frequent development of hydroureters. 12% of the irradiated sites showed luminal occlusion in segment 1, while the remaining sites displayed all 3 grades of luminal stenosis.

Radiological results

The contrast radiograms provided additional information concerning the grade and extension of the luminal stenosis or proved an occlusion as well as the development of a hydroureter. They were evaluated by measuring the luminal diameter and the longitudinal extension of the stenosed or occluded segments. In general, the contrast radiograms confirmed the histological findings at all postoperative intervals. The radiograms of the period between 2 and 16 weeks after laser irradiation (Fig. 8b) revealed a high accordance with the histologically determined grades of stenosis and with the incidence of ureteral occlusions. We observed that the length of a stenosis or an occlusion did not significantly increase between the second and sixteenth post-operative week.

Discussion

Immediately after laser irradiation, the microscopical features of the ureter wall tissues clearly demonstrate a death of cells in all wall layers of segments 1, 2 and 3. This transmural wall necrosis has also been found in other studies after Nd:YAG-laser treatment of the urinary tract (Smith *et al.*, 1984; Hofstetter and Keiditsch, 1986) and is certainly due to the high penetration depth of laser irradiation with a wavelength of 1320 nm (Sardar *et al.*, 1993). This cell death can be described as a thermonecrosis, which implies a rise of temperature above a critical value of approximately 45°C (Helpap and Grouls, 1980), resulting in a lethal cellular damage.

The ultrastructural findings suggest, that the non-cellular components of the ureteral wall layers are more resistent against the photothermic effect of Nd:YAG laser irradiation than the cellular components. This general conclusion concerning the interaction between laser light and biological tissue has also been drawn by several authors (Ben Basset *et al.*, 1976; Prince *et al.*, 1986; Zimmermann *et al.*, 1987) and is in good accordance with earlier results of our own group after laser irradiation of the rat esophagus (Schaarschmidt *et al.*, 1992; Stratmann *et al.*, 1993).

The relative thermostability of the amorphous ground substance and the collagenous fibrils is probably due to the stability of the covalent bindings of their molecules which will not disrupt at the attained temperatures. The condensation of the ground substance is electron microscopically evident and corresponds to the dense circle of fused connective tissue in the lamina propria on the light microscopical level. This condensation might be due to the formation of new cross-links between the macromolecules (proteoglycans and hyaluronic acids) resulting in reduced solubility of the ground substance so that it is less extracted by aqueous and alcoholic solutions during specimen preparation. In our view this condensation should not be regarded as a real coagulation as the term coagulation implies merely protein precipitation from an aqueous solution. The molecular structure of collagenous fibres seems to be altered by laser irradiation as they have obviously lost their ability to incorporate heavy metal ions. Consequently, they also have lost their electron microscopical cross banding pattern and appear as electron transparent spots in cross-sections.

In the connective tissue of the wall layers an occlusion of almost all blood vessel lumina was prominent. This observation has been confirmed in different tissues and specimens by several laser studies (Geboes *et al.*, 1980; Haase *et al.*, 1989; Rebeiz *et al.*, 1990). Most authors assume a formation of intravascular thrombi after endothelial damage. According to Boergen (1977),

a lesion of erythrocytes can also activate the cascade of intravascular coagulation which might be promoted by thermal plasmaprotein precipitation.

In contrast to the alterations of the extracellular matrix, the complete disintegration of cytoplasmic elements is probably due to weak binding forces between molecules of cytomembranes of cell borders, organelles and nuclear envelopes as well as between protein subunits of the cytoplasm. The photothermically induced destruction of these non-covalent bindings results in an intracellular accumulation of granulofilamentous material that was already described in epithelial cells of the human skin (Ben Basset *et al.*, 1976) and in epithelial cells of the rat oesophagus (Stratmann *et al.*, 1991, 1993) and that can be interpreted as fused or clumped fragments of cytoplasmic components.

The ultrastructural feature of cellular nuclei suggests either a destruction of the karyoplasmic matrix resulting in a chromatin collapse (pycnotic-like nuclei) or can be explained by a primary disruption of chromatin followed by a collapse or dispersion of the fragments (karyolytic nuclei) as observed in the urothelium.

The extension of the thermal wall necrosis into the peripheral laser zones of segment 2 and 3 did not reveal any histological evidence of a decreasing gradient of laser destruction in a peripheral direction. This observation supports our working hypothesis, that the ureter tissues have the property of a high thermal diffusion rate in a longitudinal direction resulting in a rapid temperature rise in the peripheral laser zones. The multiple intraurothelial vacuolation in segment 2 and 3 can be interpreted as an accumulation of a serous exudate or an inflammatory oedema respectively derived from dilated capillaries of neighbouring vital tissue.

The structural features of ureter tissues described for the immediate group are the result of a photothermal laser trauma, which induces the exudative phase and the following stages of wound healing.

The period up to the second week is marked by the resorption of necrotic material and the formation of granulation tissue, which has already been transformed into young scar tissue after 2 weeks. Simultaneously with the reparative activity, a regenerative activity of the urothelium takes place and has restored a new luminal lining after 2 weeks. This urothelial regeneration originates from vital cells which are located in more peripheral zones than segment 3. Mitotic activity appears to have been specifically stimulated by absorption of laser energy or simply by moderate rise in temperature. This mitotic activity may have been mediated by mitogens released from macrophages and thrombocytes, i.e., growth factors stimulating the proliferation of epithelial cells as well as fibroblasts and endothelium. Our findings indicate a high urothelial capability of regeneration and are consistent with observations of several authors after urothelial trauma of various origins (Schreiber *et al.*, 1969; Connolly *et al.*, 1971; Kunze *et al.*, 1979, Pensel *et al.*, 1988). In the occluded specimens of the second week group, these regenerated urothelial cells have been compressed in the centre due to centripetal growth direction of reparative scar tissue and will probably be replaced by scar tissue successively.

Between the second and the sixteenth post-operative week, all processes of wound healing have terminated apart from a maturation of the scar tissue, leading to a shrinkage of the laser treated ureter segment after 16 weeks. This conclusion is supported by our histological observation that the incidence of luminal occlusions does not increase in later postoperative stages and by the radiological evidence that the stenosis displays no further expansion in longitudinal direction after 2 weeks.

In short, our results suggest that a high expanding force of growing scar tissue in a luminal direction is a prerequisite for a successful occlusion of hollow organs. In the case of the ureter, this expanding force must exceed the hydrostatic pressure of obstructed urine in a developing hydroureter. The occlusion seems to achieve mechanical stability during maturation of scar tissue and is very likely to be a permanent one if it can be found even after 16 weeks because scar maturation can be supposed to be nearly terminated hitherto.

Clinical conclusions

Although there is no exact correlate of rectourogenital fistula in normal animal anatomy, the rabbit ureter has the advantage of a similar wall structure and geometry, as well as a luminal size in good accordance with the newborn's rectourogenital fistula. On the grounds of this study and previous experimental and clinical findings (Stratmann *et al.*, 1991, 1993; Schaarschmidt *et al.*, 1992), we assume that a laser mediated occlusion of urogenital fistulas could be conducted in future clinical treatments.

In rectourogenital fistulas due to anorectal anomaly, the probability of a permanent occlusion is even higher than in the animal model of this study since the expansion of the scar tissue is not subject to mechanical disturbances such as the increasing hydrostatic pressure of progressively obstructed urine. Therefore our experimental findings encourage further research to promote standardized clinical application.

References

Ben Basset MI, Ben Basset MO, Kaplan I (1976) A study of the ultrastructural features of the cut margin of skin and mucose membrane specimens excised by carbon

dioxide laser. J Surg Res **21**: 77-84.

Boergen K (1977) Gefäßkoagulation mit dem Argon Laser. (Vascular coagulation by argon lasers) Fortschr Med **95**: 2297-2302.

Burger RA, Gerhard CD, Bunn H, Hohenfellner R (1990) Laser assisted urethral closure in the rat: comparison of CO_2 and Nd:YAG-laser techniques. J Urol **144**: 1000-1003.

Connolly JG, Morales A, Minnaker L, Raeburn H (1971) The origin of regenerating bladder mucosa after partial mucosa stripping. Invest Urol **5**: 481-487.

Geboes K, Rutgert P, Vantrappen G, Desmet V (1980) Microscopic and ultrastructural study of chemotaxis after laser photocoagulation. Gastrointest Endosc **26**: 131-133.

Grossman HB, Schwartz SL, Konnak JW (1992) Ureteroscopic treatment of urethelial carcinoma of the ureter und renal pelvis. J Urol **148**: 275-277.

Haase KK, Steiger E, Wehrmann M, Walz R, Karsch K (1989) Effect of laser irradiation on atherosclerotic vascular segments in relation to wavelength and pulsewidth. Zeitschr Kard **78**: 701-706.

Helpap B, Grouls V (1980) Cell cinetic investigation of the thymus after different tissue lesions in parenchymal organs. Virchows Arch B Cell Pathol **34**: 277-289.

Hofstetter A, Keiditsch E (1986) Lasers for renal pelvis and ureteral tumours. Laser **1**: 75-77.

Keiditsch E (1986) Morphological fundamentals in the treatment of tumours with the Nd:YAG-laser. Eur Urol **12**: 12-16.

Kunze E, Albrecht H, Wötjen HH, Schauer A (1979) Die reparative Regeneration des Rattenurothels nach partieller Cystektomie und ihre Bedeutung für die Karzinogenese. (Reparative regeneration of rat urothelium after partial cystectomy and its significance for carcinogenesis.) J Cancer Res Clin Oncol **95**: 159-175.

Merguerian PA, Rabinowitz R (1986) Dismembered nonstented ureterostomy using the carbon dioxide laser in the rabbit: Comparison with suture anastomosis. J Urol **136**: 229-231.

Pensel J, Sommer K, Thomas S, Barretton G (1988) Functional and histological restitution in the urinary tract after Nd:YAG laser coagulation. Las Surg Med **8**: 371-376.

Prince MR, Deutsch TF, Mathews-Roth MM, Margolis R, Parrish JA, Osteroff AR (1986) Preferential light absorption in atheromas in vitro. J Clin Invest **78**: 295-302.

Rebeiz EE, Arez HT, Shapshay SM, Pankratov MM (1990) Application of pulsed and continuous wave 1.32 and 1.06 microns wavelengths of the Nd:YAG laser in the canine tracheobronchial tree: A comparative study. Las Surg Med **10**: 501-509.

Salo J, Tarri K, Nordling S, Savolainen H, Schroder T, Lehtola A, Ranniko S (1992) Healing of bladder wall after contact and non-contact Nd:YAG laser photocoagulation. Experimental study in piglets. Eur Urol **21**: 64-69.

Sardar DK, Zapata BM, Howard CH (1993) Optical absorption of untreated and laser-irradiated tissues. Las Med Science **8**: 205-209.

Schaarschmidt K, Stratmann U, Lehmann R, Willital GH (1992) The rat oesophagus: ultrastructure and clinical aspects of tissue response after 1320 nm Nd:YAG laser irradiation. Exp Toxicol Pathol **44**: 239-244.

Schmidt-Kloiber H, Reichel E, Schöffmann H (1985) Laser induced shock-wave lithotripsy (LISL) Biomed Tech **30**: 173-182.

Schreiber H, Oehlert W, Kugler K (1969) Regeneration und Proliferationskinetik des normalen und strahlengeschädigten Urothels der Ratte. (Regeneration and proliferation kinetics of normal and radiation injured rat urothelium.) Virch Arch B Cell Pathol **4**: 30-44.

Shearer P, Parham DM, Fontanesi J, Kumar M, Lobe TE, Dairclough D, Douglass EC, Wilimas J. (1993) Bilateral Wilms Tumour - Review of outcome, associated abnormalities, and late effects in 36 patients treated at a single institution. Cancer **72**: 1422-1426.

Smith J, Randall G, Dixon J (1984) Tissue effect of Nd:YAG laser photoradiation of canine ureters. J Surg Oncol **27**: 168-171.

Stratmann U, Schaarschmidt K, Lehmann R, Heinze A, Willital GH, Störmann J, Wessling G (1991) A light and electron microscopic study of the rat oesophagus following intraluminal argon laser irradiation. Acta Anat **141**: 85-89.

Stratmann U, Schaarschmidt K, Lehmann R, Willital G.H., Wessling G, Kessler T (1993) Die Gewebeantwort des Rattenoesophagus nach intraluminaler Bestrahlung mit Nd: Yag laser (1064 nm) zu unterschiedlichen postoperativen Zeitpunkten: Eine licht- und elektronenmikroskopische Studie. [The tissue response of the rat oesophagus after intraluminal radiation by Nd: YAG laser (1064 nm) at various post-operative intervals: A light- and electronmicroscopical study.] Ann Anat **175**: 95-100.

Zimmermann HD, Kraushaar J (1987) Morphological findings after renal pole resection with the laser beam in rabbits and dogs. Verh Dtsch Ges Path **41**: 477-480.

Zimmermann I, Stern J, Keiditsch E, Frank F, Hofstetter A (1987) Restitution und Reparation nach ausgdehnter gerprimärer und sekundärer mit Nd: Yag Laser Nekrose der Rattenharnblase. (Restitution and reparation after extended primary und secondary Nd: YAG laser necrosis of rat bladder. Laser **3**: 215-223.

Discussion with Reviewers

A.P. Evan: A comment is made in **Results** about the complete occlusion of almost all blood vessel lumina after laser treatment, and this change is supposed to be seen in Figure 2b. That figure is of too low a magnification to see such a level of detail.

Authors: The occlusion of almost all blood vessel lumina after laser treatment can be recognized as a very constant feature, even on the light microscopic level predominantly for the larger blood vessels, if the laser treated specimens are directly compared to the untreated controls. However, in order to make this finding more evident, we present an additional micrograph (Fig. 9).

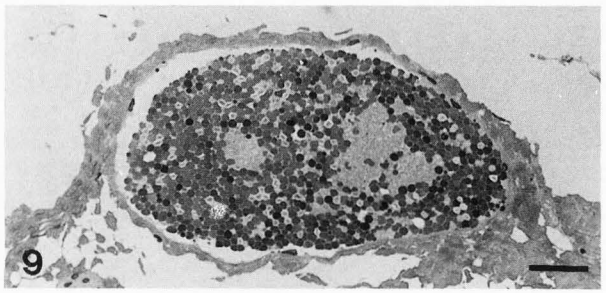

Figure 9. Light micrograph of a larger blood vessel of the tunica adventitia of a rabbit ureter immediately after laser irradiation (Nd:YAG 1320 nm 3 Watts / 8 seconds). (Note the densely packed blood cells enclosed in an intravasal thrombus occluding the vascular lumen). Bar = 70 μm.

A.P. Evan: Please expand your discussion on the mechanisms for luminal occlusion of the ureter following laser treatment.

Authors: Two weeks after laser irradiation, 37.5% of the investigated ureters showed a complete occlusion of their lumina, whereas the remaining specimens showed different grades of luminal stenosis. Our evaluations support the hypothesis that the occlusion will persist at least up to the sixteenth week, and there is no reason to assume a recanalisation in the following stages.

Basically, two different processes of wound healing occur after laser trauma of the ureter. On the one hand, an urothelial regeneration restores a new luminal lining. On the other hand, an ingrowth of granulation tissue replaces the thermonecrotic tissue and eventually leads to a stenosis or even an occlusion of the lumen. By transformation of granulation tissue into scar tissue the occlusion gains further mechanical stability.

Moreover, our observations support the assumption that an urothelial regeneration does not disturb a luminal occlusion since the epithelial cells are supposed to be compressed by expanding granulation tissue and will be replaced by connective tissue after atrophy due to pressure. Against that, an obstruction of urine flow will dilate the lumen and result in the development of a hydroureter.

A.P. Evan: The reviewer is still not sure how the data collected in this study will be used. Did the authors answer their question listed in **Introduction**?

Authors: The answer to the above mentioned question of future clinical applicability of the laserendoscopic technique has been given in **Clinical Conclusions**. Of course, this study should be understood as an applied basic research work in preparation of future clinical studies on laser endoscopy; nevertheless, the overall important question, whether a laser-endoscopic occlusion of urinary hollow organs is feasible at all, has been answered definitely by proving the possibility of luminal occlusion in this study. A laser-mediated occlusion of hollow organs in two further animal models has already been reported by our group for the rat esophagus (Schaarschmidt *et al.*, 1992) and the piglet esophagus (Stratmann *et al.*, 1995).

Reviewer II: In the human ureter, neither "lenticular vesicles" nor "dark granules" are prominent. Can the authors provide references as to what the structures represent?

Authors: According to Jost *et al.* (1989), the surface layer cells of the normal human urothelium contain electron-lucent, round or fusiform (= lenticular) vesicles with varying length (0.2-0.5 μm) and varying diameter (0.04-0.2 μm). Of course, these vesicles are supposed to be a typical feature also in the urothelium of other mammalian species due to their functional significance for surface enlargement during luminal extension. Secondly, the dark granules might represent particularly electron-dense lysosomes but cannot be characterized definitely by only morphological data.

Reviewer II: In the clinical setting, how will the authors determine the appropriate dose and time of laser treatment for fistula occlusion?

Authors: The first step is to measure the absorption rate of freshly dissected ureter segments and to record the temperature of the ureter wall by a thermocamera after irradiation with the investigated experimental parameters. In the second step these data have to be compared with the data obtained after irradiation of freshly dissected fistula after irradiation with identical parameters. In case of an acceptable correspondence the values of dose and time can be transferred from the experimental model to the clinical setting.

Indeed the principle of an endoscopic laser occlusion

of fistulae has already been applied successfully by Schmittenbecher *et al.* (1992) in newborn children suffering from congenital tracheoesophageal "H-fistula."

Additional References

Jost SP, Gosling JA, Dixon JS (1989) The morphology of normal human bladder urothelium. J Anat **167**: 103-115.

Schmittenbecher PP, Mantel K, Hofmann U, Berlien HP (1992) Treatment of congenital tracheoesophageal fistula by endoscopic laser coagulation: preliminary report of three cases. J Pediatr Surg **27**: 26-28.

Stratmann U, Schaarschmidt K, Lehmann RR, Schürenberg M, Willital GH, Berens A (1995) The morphological tissue response of the piglet oesophagus to experimental irradiation by the Nd:YAG laser (1320 nm). J Anat (in press).